JOURNAL OF PROPULSION AND POWER
Vol. 22, No. 6, November–December 2006

Recombination of Electrothermal Plasma and Decomposition of Plasma-Exposed Propellants

Jianquan Li,* Thomas A. Litzinger,† Malay Das,‡ and Stefan T. Thynell†
The Pennsylvania State University, University Park, Pennsylvania 16802

DOI: 10.2514/1.17685

Information about species involved in initiating ignition of propellants by electrothermal plasma is critical to determining any chemical effect on the enhancement of electro-thermal-chemical gun performance. An experimental study using a triple-quadrupole molecular beam mass spectrometer was conducted to measure species from plasma recombination and from plasma-induced decomposition of propellants (JA2 and M43). The mismatch between the plasma pulse and the sampling time requirement by the mass spectrometer makes direct probing plasma species difficult, requiring the use of a plasma-holding chamber to prolong the event for sampling. The secondary jet evolving from the holding chamber should represent the nature of the plasma jet as it propagates through the propellant bed in actual electro-thermal-chemical applications. Recombination species that can be consistently detected are C_2H_4, C_2H_3, C_2H_2, CH_4, CH_3, H_2, and H for a plasma produced within a polyethylene capillary. NO, CO and CO_2 are also detectable if sufficient air is present in the chamber or using a Lexan capillary. Species measurements of JA2 and M43 indicate the formation of NO and H_2CO during impingement by the jet, which are typical "dark-zone" species observed for these propellants.

Nomenclature

i_1	=	electric current flowing through the capillary plasma
i_2	=	electric current flowing parallel to the capillary plasma
L_{n-s}	=	distance between nozzle exit to propellant sample
p	=	pressure
t	=	time
x_p	=	distance between nozzle exit to stagnation plate
x_M	=	location of Mach disk

Introduction

THE electro-thermal-chemical (ETC) propulsion concept has been the subject of substantial research activities [1–8]. This propulsion concept, which uses electrically generated plasma for ignition, has potential application in both medium- and large-caliber weapon systems. Results from laboratory experiments and actual firing tests have revealed that the use of ETC plasma ignition can offer several attractive benefits over conventional chemical powder ignition, such as precision ignition in terms of shorter and more reproducible ignition delay [9], mitigation of gun performance sensitivity to ambient temperature [10,11], better controlled propellant mass generation rates [12], and the ability to reliably ignite low vulnerability ammunition propellants [13] and high loading density propellant charges [14,15]. However, optimization of the ETC igniter design relies on a clear and complete understanding of the underlying fundamentals that account for these observed benefits.

This paper presents results from recent experimental work on species measurement during the recombination of plasma species and the interaction of plasma with a double-base propellant, JA2, and a nitramine composite propellant, M43. The objective of this work is to gain insights from parametric studies that will contribute to the formulation of a complete understanding of chemical effects in the enhancement of ETC gun performance.

Received 13 May 2005; revision received 17 May 2005; accepted for publication 27 January 2006.

*Postdoctoral Scholar, Department of Mechanical and Nuclear Engineering. Member AIAA.
†Professor, Department of Mechanical and Nuclear Engineering. Senior Member AIAA.
‡Research Assistant, Department of Mechanical and Nuclear Engineering. Member AIAA.

Experimental Approach

The *plasma generator* has been described in detail elsewhere [16–18], and hence a summary is given herein. As shown in Fig. 1, the pulse forming network is based on a resistance-inductance-capacitor circuit, which is mainly composed of an energy storage component that consists of two high-voltage fast-discharge capacitors connected in parallel to yield a total capacitance of 192 μF, pulse-shaping components including a 20 μH inductor and a crowbar diode, and a floating high-voltage mercury switch (ignitron) as the trigger unit. The capacitors can be charged up to 10 kV corresponding to maximum energy storage of 9.6 kJ. The plasma chamber consists of a capillary liner, a fine metallic wire, electrodes, and other conducting or nonconducting housing hardware. The capillary liner is typically made of either high-density polyethylene (PE, $[C_2H_4]_n$) or polycarbonate (Lexan, $[C_{16}H_{14}O_3]_n$), which is machined to have a bore length of 26 mm and a typical diameter of 3.2 mm. The electrodes are made of erosion-resistant material, elkonite, a copper-tungsten alloy (30% Cu, 70% W). Inside the capillary is a fine copper filament (0.08 mm) connecting the electrodes and serving as the discharge initiator. After being formed immediately upon triggering the ignitron, the generated plasma flows through a nozzle that has typical dimensions of 3.2 mm [inner diameter (ID)] and 13.5 mm (length) into open air or a closed chamber.

The *mass spectrometer* is also depicted in Fig. 1, which is an Extrel triple-quadrupole mass spectrometer (TQMS) with two sampling schemes: one using tubular microprobes and the other using a cone-skimmer configuration. In microprobe sampling, two quartz probes are usually used. The primary probe has dimensions of 50 mm (length), 2 mm (ID) and 3.2 mm [outer diameter (OD)]; its front end is fabricated by pulling during torch heating to form a conical tip, which is then ground to open an orifice of about 30 μm in diameter. The secondary probe (not shown in the figure) is 120 mm (length), 4 mm (ID) and 6.35 mm (OD). The orifice of the secondary probe is about 100 μm, which is placed behind the primary probe with a gap of $\sim$1.0 mm. The advantages of the microprobe sampling are better spatial resolution and larger strength to take higher pressures in the test chamber. In the cone-skimmer scheme, a cone-shaped sampler is used, which is 20 mm long and has an orifice of 100 μm at its apex. The selection of relatively large included angles (interior 50 deg and

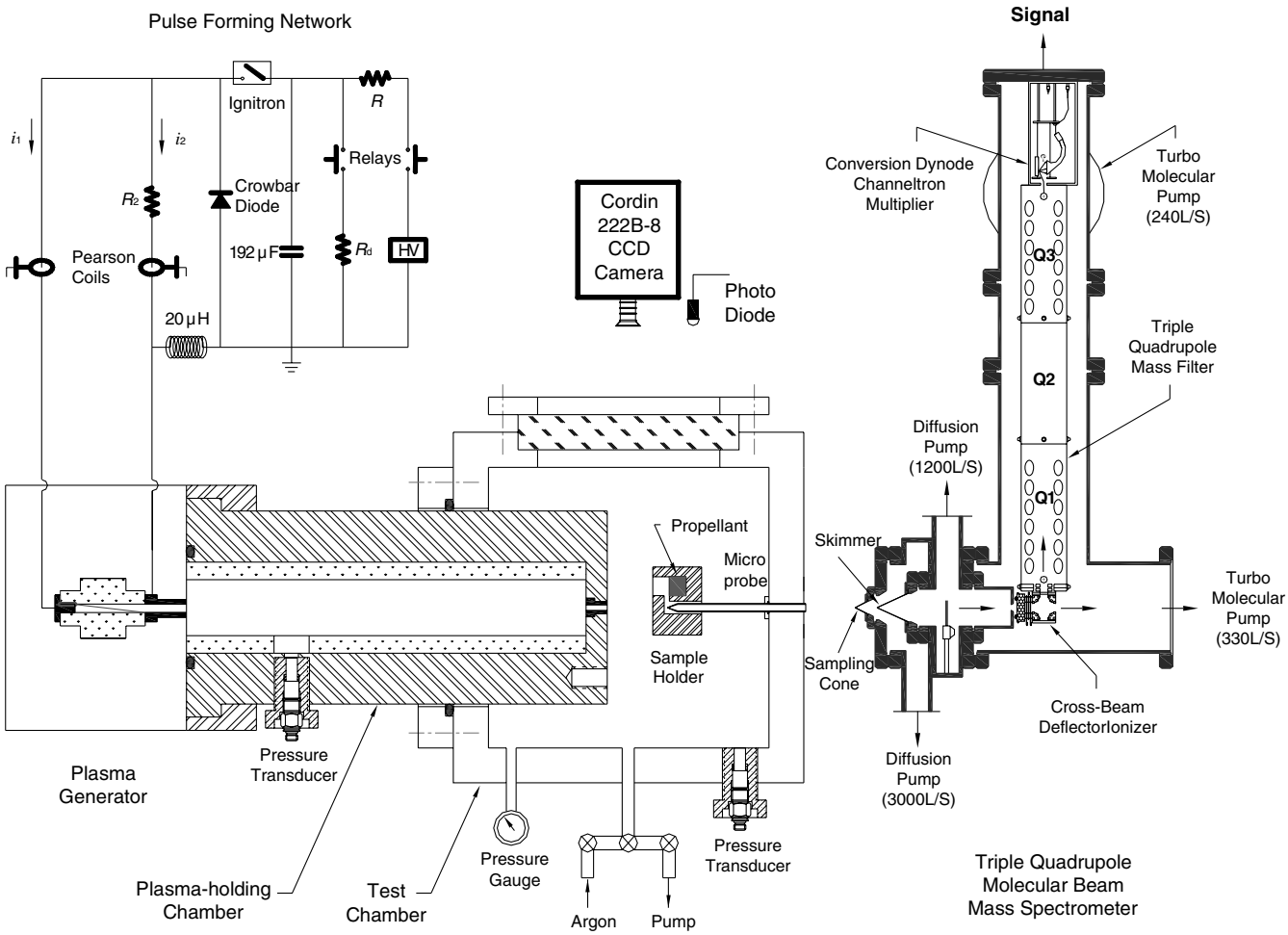

Fig. 1 Setup for species measurement in a closed environment.

exterior 55 deg) is expected to allow a "free" expansion for the supersonic jet developing inside. The skimmer is comparatively large both in length (50 mm) and in orifice diameter (1.5 mm), and has a 55 deg interior angle and a 60 deg exterior angle. Both the sampling cone and the skimmer were obtained from Beam Dynamics, Inc. A plating technique is employed to fabricate them using nickel. While maintaining the very sharp tips ($\sim$5 μm), double thickness of wall and additional rhodium plating were applied for improved mechanical strength and better protection from corrosion. Specially designed fixtures were used to hold the cone and the skimmer in place onto standard flanges for mounting to the vacuum chambers. The cone-skimmer distance is adjustable by using spacers for better beam performance. The use of cone-skimmer scheme enables molecular beam sampling to directly probe unstable intermediate species such as radicals and ions, which is desirable for applications like plasma species measurements.

Custom designed vacuum chambers fabricated in MDC Vacuum Products, Inc. were included in the vacuum system in a way that the flight distance from the sampler tip to the ionizer is kept as short as possible to achieve a better beam intensity. A three-stage differential pumping system is established by using various vacuum pumps to meet the pumping-out requirement imposed by the orifices. A DIP3000 diffusion pump (3000 liter/s) with a D25B rotary vane backing pump (25.7 m^3/h) both purchased from Leybold Vacuum Products, Inc., is used in the source chamber (or expansion chamber) as the first pumping stage ($10^{-3} \sim 10^{-4}$ torr). The second stage formed in the beam chamber (behind skimmer or secondary probe) is supported by another diffusion pump (Varian VHS4, 1200 liter/s) with a mechanical backing pump (Varian SD301, 15 m^3/h), yielding a $10^{-5} \sim 10^{-6}$ torr vacuum condition. Water-cooled baffles are used for both diffusion pumps to prevent backstreaming of vapor from the pump oil (DC 704 silicone oil). The third stage ($\sim 10^{-7}$ torr) is evacuated by two turbo molecular pumps (330 and 240 liter/s) from Pfeiffer Vacuum, Inc.

The ionizer is an Extrel cross-beam-deflector ionizer,[§] which is a combination of an axial ionizer mounted perpendicularly to the mass filter axis and a small quadrupole deflector energy filter. The energy-filtering capability of this ionizer provides great improvement in its sensitivity, because the deflected beam can get energies up to hundreds of electron volts, which is readily accommodated simply by tuning the lenses of the energy filter. The right angle design is expected to dramatically increase signal-to-noise by removing the unwanted components of the sample, such as photons, energetic neutrals, and even particulates, because they are directly pumped away by the turbopump behind the ionizer. This configuration also helps to reduce contamination of the quadrupoles and the detector for better performance in corrosive and high-particulate applications, particularly in the ETC plasma sampling, where a considerable amount of soot is produced.

Initial efforts in plasma species measurements were made to directly probe the species of plasma jets during freely expanding in open air. However, it was soon found that the temporal mismatch between the plasma pulse ($\leq$ 0.3 ms) and the requirement for sampling duration by the mass spectrometer ($\gg$ 0.3 ms) makes direct sampling from the jet practically impossible. Furthermore, the presence of metallic particles in the plasma jet [19] renders difficulty in protecting the sampler orifice from enlargement or even damage, which is especially true for the cone-skimmer configuration. To circumvent these difficulties, a plasma-holding chamber is used, as shown in Fig. 1.

[§]Data available on-line at http://www.extrel.com [cited 12 April 2005].

The *plasma-holding chamber* is a small cylindrical chamber with one end attached to the plasma generator and the other extending to a test chamber and interfacing with the sampling probe through a small nozzle of a 1 mm orifice to slow down the flow out of the chamber. Tubular sleeves of different sizes and/or materials were inserted in the holding chamber to vary its actual volume. The experiments involved the use of metal (aluminum) and nonmetal (PE or Lexan) materials. The test chamber, which interfaces with the mass spectrometer through a flange that holds the primary microprobe or the cone, has a $10 \times 10 \times 10$ cm internal volume and is equipped with a 6.5 cm circular window for photography.

The plasma-holding chamber coupled with a closed test chamber is considered as a promising setup in that the holding chamber prolongs the sampling duration through sampling a secondary jet from it rather than the primary plasma jet from the plasma generator; the closed test chamber can create a subatmosphere condition by connecting to a vacuum pump; this subatmosphere condition increases the absolute fraction of the jet species in the whole plume drawn into the sampling probe. Also, because the holding chamber and the test chamber are connected as a whole closed system, it is very convenient to purge the chambers with desired background gases to investigate the effects of ambient conditions on species information of the jets.

A sample holder was used to allow measurements of species near the plasma-propellant interfacing region. The sample holder has a short passage that connects the propellant and the probe tip. This configuration increases the likelihood of detecting species near the propellant surface. The sample holder was removed when species measurement was conducted with plasma alone.

Other supplementary measurements include pressure histories in the holding chamber, images of the secondary jet, and diode signals that monitor the discharge process of the secondary jet. These measurements are an aid in interpreting the species data. The setup for these measurements is also illustrated in Fig. 1.

Results and Discussion

When using the plasma holding chamber, a concern is raised about whether the secondary jet issuing from the holding chamber would be substantially different from the primary jet from the capillary/nozzle. Such a concern is based on the consideration that, after the plasma enters the holding chamber, its temperature may significantly drop due to heat transfer to chamber walls. For this reason, the species measurement was done mostly with PE or Lexan inserts (depending on the material of the capillary used in a test), and the net volume of the holding chamber was made as small as possible. In general, these tubular inserts have dimensions (both inner diameter and length) five times larger than those of the capillary.

Figure 2 shows typical results of the chamber pressure and the diode signal. Compared with the plasma pulse of ~0.3 ms, the duration of the secondary jet was substantially extended, to 50–60 ms. In addition, the resulting chamber pressure falls within a range comparable to the capillary plasma dynamics during the ignition phase of the interior ballistic cycle [20]. Figures 3a and 3b present images of the primary jet and the secondary jet where the "submerged" sampling probe is clearly visible. Different CCD gain settings were used for these images to obtain comparable brightness. The images at 0.09 ms show that the secondary jet at early times still exhibits a shock cell structure similar to the primary jet, but this structure soon disappears within a few milliseconds.

Elemental Compositions in Plasma

Although the capillary plasma is initiated by vaporization of the exploding wire and sustained by ablation of the capillary wall material, the wire and the capillary are not the only sources for the plasma mass. The total mass of the plasma jet is composed of contributions from several sources, which, in addition to the trigger wire and capillary, also include the end electrode (anode), the nozzle (cathode), and the air that is initially trapped in the capillary.

Generally, because the nozzle undergoes intense radiative and convective heating by the plasma flowing through it at high

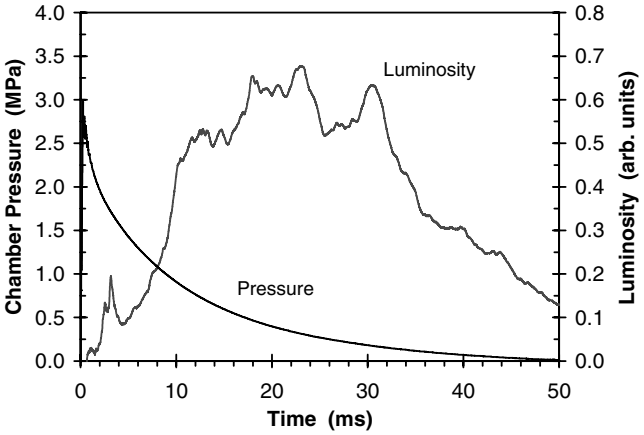

Fig. 2 Pressure in holding chamber and luminosity of secondary jet (4 kV, PE).

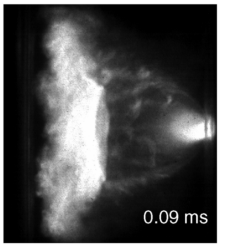

a)

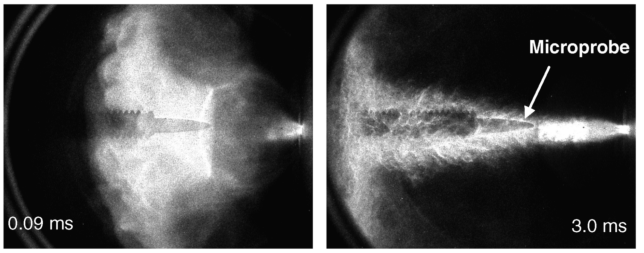

b)

Fig. 3 Images of a) primary jet and b) secondary jet.

velocities, ablation of its wall material provides a major fraction to the total plasma mass. As a result, the mass of metallic particles contributes a major part to the total mass of the plasma jet as shown in Fig. 4a. However, by mole fraction, it is the elements (H and C) from the capillary that dominate over all other species as indicated in Fig. 4b. Therefore, the capillary mass loss due to ablation is of great importance to the chemistry of the plasma.

Recombination of Plasma Species

Spectroscopic measurements by Kohel et al. [21] show that the plasma temperature in the region of upstream of the Mach disk is about 23,400 K at 30 μs after the pulse discharge begins for a charging voltage at 5 kV. Inside the capillary, the temperature must be even higher. At these temperatures, the plasma is almost completely composed of atomic species, mainly including C, H, C^+, H^+ and electrons for PE material, and with the addition of O and O^+ for Lexan plasma. After entering the holding chamber, recombination of these atomic species takes place as the temperature drops due to a combination of heat transfer to walls and turbulent mixing with background gases. How quickly or to what level the temperature would drop in the holding chamber, a question similar to what is the temperature when the plasma reaches the propellant

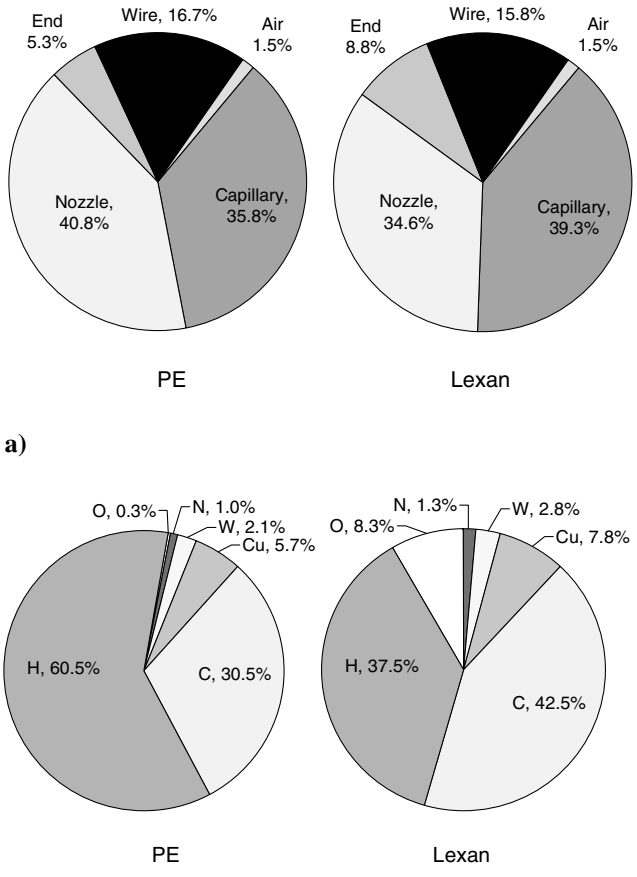

Fig. 4 Contribution to primary jet (4 kV, 3.2 mm capillary): a) by mass source, b) by elemental composition.

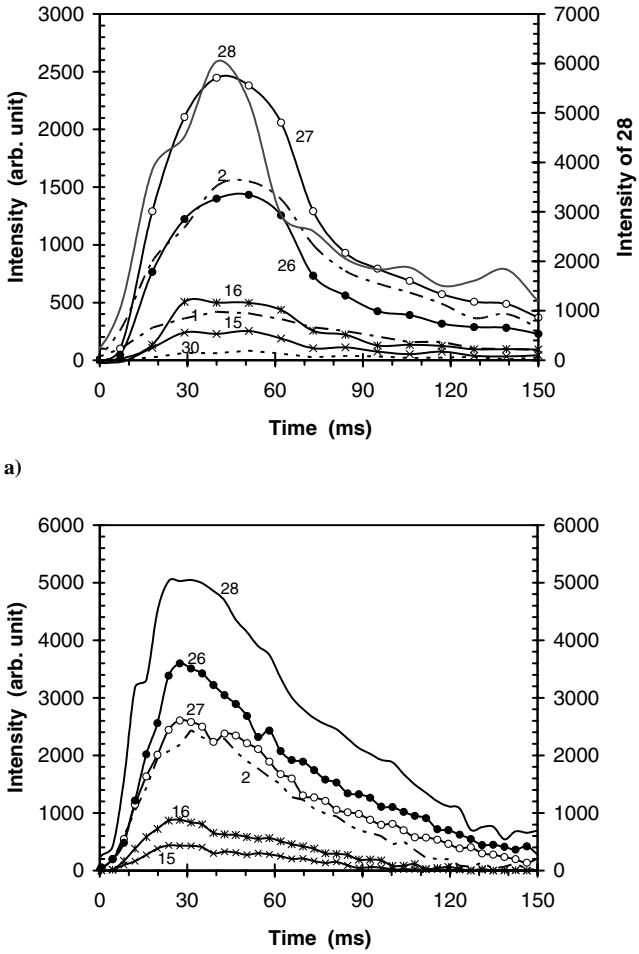

Fig. 5 Recombined species from 4 kV PE plasma with initial background a) 1 atm air and b) 1 atm argon.

surface in actual applications, determines the recombined products in the secondary jet.

The sampling was initially performed through scanning over all possible species resulting from recombination of the plasma species. The variation in test conditions included plasma source material, location of sampling probe in the jet, plasma energy, and initial background conditions. For all conditions considered, the recombined species that can be consistently detected are found to have mass-to-charge ratios (m/z) of 28, 27, 26, 16, 15, 2, and 1. In some tests, species at m/z of 44, 30, and 25 also appeared, but their signals are usually small and they are not consistently detectable.

Figure 5a displays a result of microprobe sampling, where detected species are plotted against the sampling time. In addition to those species that can be detected by the mass spectrometer, another major product during recombination is soot, which consistently appears in considerable amounts for each test and under all conditions. It was found that Lexan plasma produces less soot than PE plasma, which is an outcome of the difference in their elemental compositions. Except for this difference, the jet species from these two materials are quite similar.

Experiments using the cone-skimmer configuration were also carried out, but unfortunately, its extremely thin-edged orifice (5 μm) was significantly enlarged after impingement by the jet. Another alternative sampler employed in this work was a disk, which has dimensions of 10 mm in diameter and 1 mm in thickness. The orifice of the disk can take higher pressures than that of the cone, but enlargement due to impingement still occurs. Moreover, the detected species are basically the same with those by using the tubular microprobes. For these reasons, most of the experiments were conducted using the microprobes.

In this work, the energy for electron impact (EI) applied to the ionizer was kept at 22 eV, which is not sufficient to produce doubly ionized species. Therefore, identification of the detected species based on the values of mass-to-charge ratio (m/z) is straightforward in general, and the results are summarized in Table 1.

Differentiation of species that have the same m/z value was enabled through an analysis of daughter ions using a MS/MS method by running the TQMS in "daughter mode" [16], or through purging the holding chamber with desired background gases. For example, identification of species at m/z of 28, which corresponds to three species (C_2H_4, CO, and N_2), can be easily done by purging the test chamber with argon to eliminate N_2 and CO for PE plasma, which is void of oxygen. For Lexan plasma, daughter ions are needed to differentiate CO and C_2H_4. A similar procedure was used to differentiate species at m/z of 30. A typical result of PE plasma with argon as the background gas is shown in Fig. 5b, where the signal for m/z at 28 can only be ethylene, C_2H_4. Intensities of m/z at 30 and 1 are small, and thus not included in the plot.

Before any further discussion, a question that needs to be addressed first is whether the detected species actually exist in the secondary jet. Such a concern is that the smaller species could come from fragmentation of larger species, for example, C_2H_3 (27) from C_2H_4 (28) due to the loss of 1 H as a result of electron impact in the ionizer, or that the larger species could be formed through recombination of smaller species after, rather than before, entering the microprobes.

One way to address this is to refer to the standard mass spectra for those species that produce fragments during electron impact. Figure 6 shows the standard mass spectra for hydrogen (H_2), methane (CH_4), acetylene (C_2H_2), and ethylene (C_2H_4). As shown in the figure, fragments of varying intensities do exist for these species,

Table 1 Recombined species from PE/Lexan plasma in 1 atm air condition

m/z	44	30	28	27	26	25	16	15	2	1
Ions	CO_2^+	$C_2H_6^+/NO^+$	$C_2H_4^+/CO^+$	$C_2H_3^+$	$C_2H_2^+$	C_2H^+	CH_4^+	CH_3^+	H_2^+	H^+
Species	CO_2	C_2H_6/NO	C_2H_4/CO	C_2H_3	C_2H_2	C_2H	CH_4	CH_3	H_2	H

especially for ethylene and methane. For hydrogen, the fragment (H) is very small and thus can be neglected.

However, these standard mass spectra are obtained with EI at 70 eV, which is considerably higher than the value (22 eV) used in the plasma test. The resulting difference in electron energy may cause changes in the EI process and thus produce different fragments. To investigate this effect, tests were run to get the mass spectrum of C_2H_4 by setting the EI at 22 eV and all other electronic parameters of the mass spectrometer the same with those used for the plasma test. The result is presented in a similar way to that employed in Fig. 6 and shown in Fig. 7, in which relative abundance represents the number of times an ion of a certain m/z value strikes the detector. Determination of relative abundance is obtained by assigning the most abundant ion ($C_2H_4^+$) a relative abundance of 100%, and all other ions are shown as a percentage of that most abundant ion. Compared with the mass spectrum of C_2H_4 at EI of 70 eV, the relative abundances for 26 ($C_2H_2^+$) and 27 ($C_2H_4^+$) at 22 eV significantly drop from 53 to 26%, and 62 to 29%, respectively, which is about 50% reduction in the relative abundance for each ion. In addition, smaller fragments seen at EI of 70 eV do not appear at 22 eV.

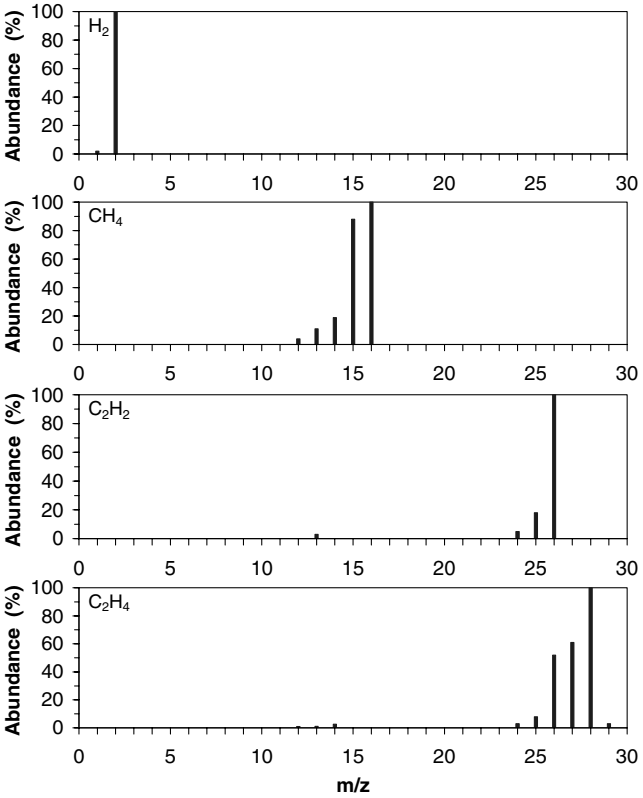

Fig. 6 Standard mass spectra at EI of 70 eV [22].

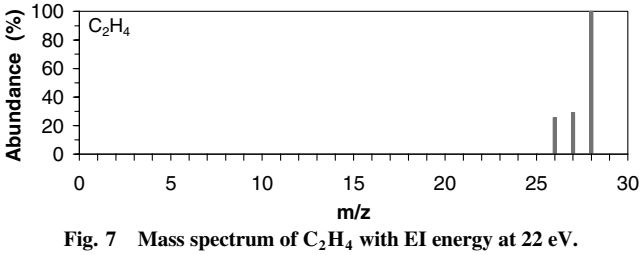

Fig. 7 Mass spectrum of C_2H_4 with EI energy at 22 eV.

The comparison made for ethylene will help to estimate the fragments of 16 (CH_4) and 26 (C_2H_2) at 22 eV from their corresponding standard mass spectra obtained at 70 eV, because experiments at 22 eV for these standard gases were not conducted at this time. The estimated values are listed in Table 2, where species listed in shaded boxes are the parent ions. Also included in the table are the relative abundances for the same species detected in plasma tests. Compared with the calibration data, the relative abundances of C_2H_3 (27), C_2H_2 (26), C_2H (25), CH_3 (15), and H (1) detected in the secondary jet are all larger than those resulting from fragmentation of their parent ions, which means that these species are actually present in the jet.

It should be noted that the calibration test for the mass spectrum of ethylene was run in room temperature, which is much lower than the temperature of the secondary jet. However, it is likely that the temperature of the secondary jet is less than 5000 K judged by the pressure drop in the holding chamber. This temperature difference corresponds to a $\sim$0.4 eV increase in the thermal energy of the hot molecules of C_2H_4. Compared with the 22 eV EI energy, this difference is very small, and its effect on the fragmentation can thus be neglected.

As to the second concern about possible recombination of smaller species to form larger ones in the microprobes, a detailed discussion can be found in [16], which indicates that recombination reactions in the probe is extremely small, for example, only about 0.03% increase in C_2H_4 for a duration of 1.0 ms, which is much longer than its residence time, 0.2 ms, in the probe. For all other species, their increases in intensity due to recombination in the probe are even smaller. Furthermore, the similarity of the species data obtained in microprobe sampling with those from molecular beam sampling using the cone-skimmer (less chance for collision/recombination than in the tubular probe) also suggests that recombination reactions would not prevail in the probe. In view of the preceding analysis, it is likely that all the species detected are present in the secondary jet.

Effect of Sampling Location

All the species measurements were conducted along the jet centerline. Variations were made in the sampling location, x_p, which is the distance from the probe orifice to the secondary nozzle exit, to determine if there are any changes in composition with distance. Selection of sampling locations was considered to include the regions both upstream and downstream of the location of Mach disk in the jet, although the Mach disk has a short lifetime (less than 1.0 ms) compared with the jet duration. For conditions typically encountered in the species measurements, the value of x_M varies between 20 and 30 mm. Experiments were performed at x_p ranging from 5 to 40 mm in a 5 mm increment, and the results are presented in Fig. 8, in which the relative intensities of the species expressed as ratios over the intensity of mass 28 are plotted against probe locations. The intensity of N_2 has been subtracted from that of mass 28, so mass 28 corresponds to C_2H_4 and CO. The intensities for all species considered are averaged over the time period during which the jet issues from the holding chamber.

It appears that there is only a slight dependence of the relative abundances of these species on the probe location, with higher values occurring within 20 mm $\leq x_p \leq$ 30 mm. Such a slight dependence suggests that recombination reactions are nearly finished in the chamber.

Effect of Initial Ambient Condition

The inner wall material of the plasma holding chamber used either PE or Lexan for most of the species measurements. The initial

Table 2 Major fragments in collision-induced dissociation of C_2H_4, C_2H_2, CH_4, and H_2

Species	C_2H_4	C_2H_3	C_2H_2	C_2H_2	C_2H	CH_4	CH_3	H_2	H
m/z	28	27	26	26	25	16	15	2	1
Ions	$C_2H_4^+$	$C_2H_3^+$	$C_2H_2^+$	$C_2H_2^+$	C_2H^+	CH_4^+	CH_3^+	H_2^+	H^+
Abundance, %, at 70 eV [22]	100	62	53	100	19	100	89	100	2
Abundance, %, from calibration (22 eV)	100	29	26	100	≤10[a]	100	≤45[a]	100	≤1[a]
Abundance, %, from plasma (22 eV)	100	70[b]	43[b]	100	16[b]	100	80[b]	100	33[b]

[a]Estimated value. [b]Maximum value.

purpose of using these materials was to reduce the temperature drop of the plasma after entering the holding chamber so as to slow down the recombination process. During the tests, it was found that when these materials are used, the holding chamber, more precisely the PE/Lexan insert, essentially serves as an extension of the plasma capillary. Mass loss due to ablation was found to occur from the inner wall of the PE or Lexan insert during each test, and the amount is about three to five times of the mass loss from the capillary. Because the plasma temperature is around 23,000 K [20] when entering the chamber, it is likely that the ablated mass undergoes a process similar to what is occurring in the capillary: ablation, vaporization, dissociation, and ionization, producing additional plasma to supplement the primary plasma. It was also found that the wall ablation extends to a distance about 50 mm from the primary nozzle exit and the closer to the nozzle, the more severe the ablation. Therefore, recombination reactions in the holding chamber (130 mm long) likely start to prevail in a region beyond this distance.

Whether the detected species come from plasma recombination or from dissociation of ablated chamber wall material is a question that needs to be addressed. To that end, an aluminum (Al) insert of the same dimensions with PE/Lexan inserts was used. The resulting chamber pressures, as shown in Fig. 9, indicate the combined effect of differences in the mass of plasma and in heat transfer from plasma to chamber walls when using Al in comparison with PE as chamber material.

Figure 10a provides a typical result of recombination species using the Al chamber, where the initial condition before firing the plasma is 1 atm air. Under such a condition, the amount of air in the capillary and the holding chamber weighs about 10 times of that of the capillary ablation mass, or 9.5 times on a molar basis. Consequently, it is not surprising that intensities of the recombined species drop substantially, as can be seen in the figure, where the intensities for species of m/z at 27, 26, 16, 15, 2, and 1 are all in the noise level.

What is different from the tests using PE or Lexan chambers is the appearance of species of m/z at 30, 28, and 18. Note that the intensity of N_2 has been subtracted from that of mass 28. Clearly, mass 18 is H_2O. Mass 28 must come from CO, because C_2H_4 is very small, judged by the absence of C_2H_3 and C_2H_2. Chemically, mass 30 can be C_2H_6 or NO, but further tests in daughter mode confirmed that it is NO. This result indicates that mixing of the plasma species with the air initially contained in the holding chamber is occurring, and nitrogen and oxygen take part in the recombination process occurring simultaneously in the plasma, and finally form CO, NO, and H_2O. The CFD modeling result by Nusca and McQuaid [23] also suggests the formation of these species in the plasma expansion in open-air causing mixing layers that have combined the plasma species with air leading to chemical reactions.

To detect the recombined plasma species, additional experiments were conducted in a subatmosphere ambient condition, that is, before firing the plasma, the test chamber was pumped down to create a low background pressure. In a low-pressure background condition, the mole fractions of jet species are increased relative to the background gases that are drawn into the sampling probe, and the multiplier of the mass spectrometer can be adjusted to higher gains, so that the signal intensities of the jet species are increased.

Figure 10b presents a result with an initial background pressure at 0.01 atm. As expected, the intensities of masses 30 and 18 become very small due to the reduced amount of N_2 and O_2, which confirms that they are NO and H_2O, respectively. The intensity of mass 28 also decreases due to less oxygen available to form CO. Compared with the result in 1 atm air [Fig. 10a], another significant change in Fig. 10b is the appearance of the recombined plasma species, including almost all the species detected in tests using PE or Lexan chambers under 1 atm air condition.

To further investigate the effect of initial chamber condition, additional tests were run using Lexan or PE as both the chamber and capillary material at 0.01 atm conditions. Typical results are presented in two figures: Fig. 11, which shows the effect of capillary/chamber materials at 0.01 atm, and Fig. 12, which compares the effect of initial chamber pressures for Lexan and PE materials. As shown in Fig. 11, compared with the Al chamber, PE or Lexan chambers, owing to the increase in plasma mass from ablation of the

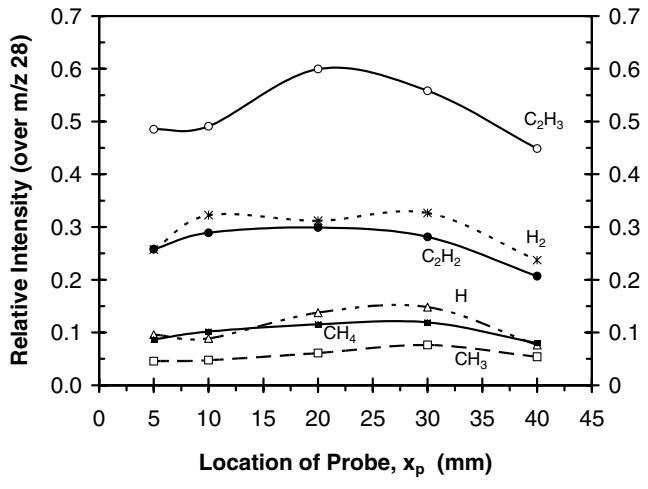

Fig. 8 Effect of sampling location (4 kV PE, 1 atm air).

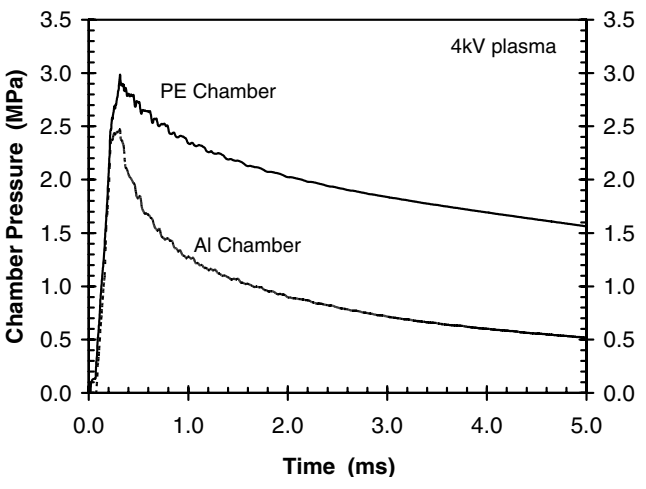

Fig. 9 Variation in chamber pressure.

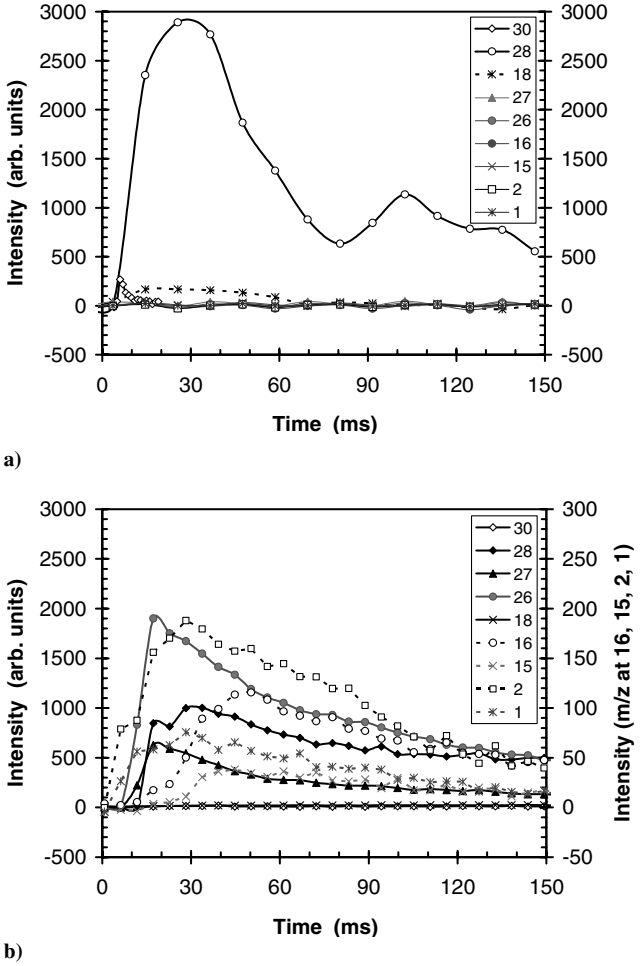

Fig. 10 Species of 4 kV PE plasma using Al chamber with initial background a) 1 atm air and b) 0.01 atm air.

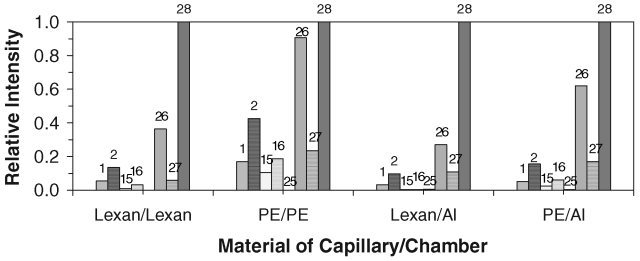

Fig. 11 Effects of chamber material on recombination products (5 kV, initial background 0.01 atm air).

chamber wall material, give higher species intensities relative to the intensity of species at m/z 28 ($CO + C_2H_4$). Such a difference between the Lexan chamber and the Al chamber is relatively small, because Lexan also contributes to the formation of CO.

In Fig. 12, when the initial condition is changed from 1 to 0.01 atm, the major changes are an increase in m/z 26 (C_2H_2) and a decrease in m/z 27 (C_2H_3), and these changes are substantial for both PE and Lexan materials. This is an indication that the initial air in the chamber affects the final recombination products.

Effect of Plasma Energy

A series of experiments were performed to investigate the effect of input electrical energy on the recombination of plasma for charging voltages ranging from 3 to 6 kV. The plasma chemistry was varied through the use of different materials, PE or Lexan, for the capillary and the holding chamber insert. The typical results from these plasmas are presented in Fig. 13, where the relative intensities of

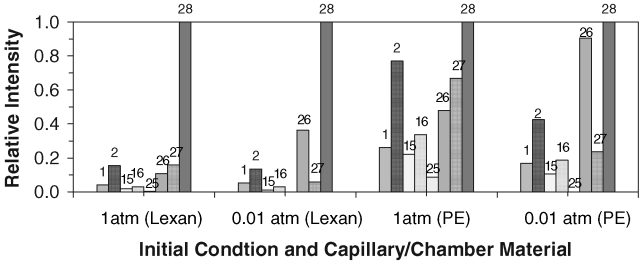

Fig. 12 Effect of initial chamber conditions on plasma recombination (5 kV).

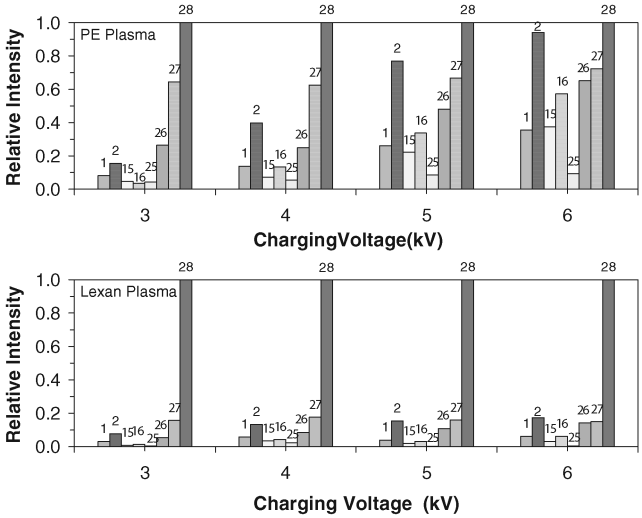

Fig. 13 Effect of charging voltage on plasma recombination ($x_p = 40$ mm, initial background 1 atm air).

smaller species expressed as ratios over the intensity of m/z 28 are plotted against four charging levels of 3, 4, 5, and 6 kV, corresponding to electrical energies of 0.86, 1.56, 2.40, and 3.46 kJ. Again, the intensities for all species considered are averaged over the time period during which the jet issues from the plasma holding chamber.

It is clearly revealed in the figures that an increase in charging voltage increases the relative intensities of smaller species for PE plasma, which is especially true for H_2 (2), CH_3 (15), and CH_4 (16). This trend is an indicator that the plasma energy strongly affects the recombination process, showing that smaller molecules become increasingly dominant in the jet as more energy is deposited into the plasma. The abundance in hydrogen atoms and molecules may be a crucial factor in performance enhancement observed in ETC guns. For Lexan plasma, the energy effect is also evident, and the general trend still applies that higher plasma energies increase the relative intensities of smaller species.

In comparison with the PE plasma, a substantial difference is found for the Lexan plasma, which is that the relative intensities of species at $m/z \leq 27$ become significantly lower; or in other words, the species of m/z at 28 dominates over all other species in the jet. This is reasonable given that fact that Lexan ($[C_{16}H_{14}O_3]_n$) contains oxygen and thus has more CO formed in the recombination contributing to mass 28.

Species from Plasma-Propellant Interaction

Propellant species measurements were done with JA2 and M43. The propellant sample was placed about 15 mm downstream of the secondary nozzle exit, and a 1.5 mm hole provides a passage for any products resulting from plasma-propellant interaction to reach the microprobe orifice for sampling. Typical results are presented in Fig. 14. In addition to the recombined species from the plasma, two other species coming from decomposition of the propellant

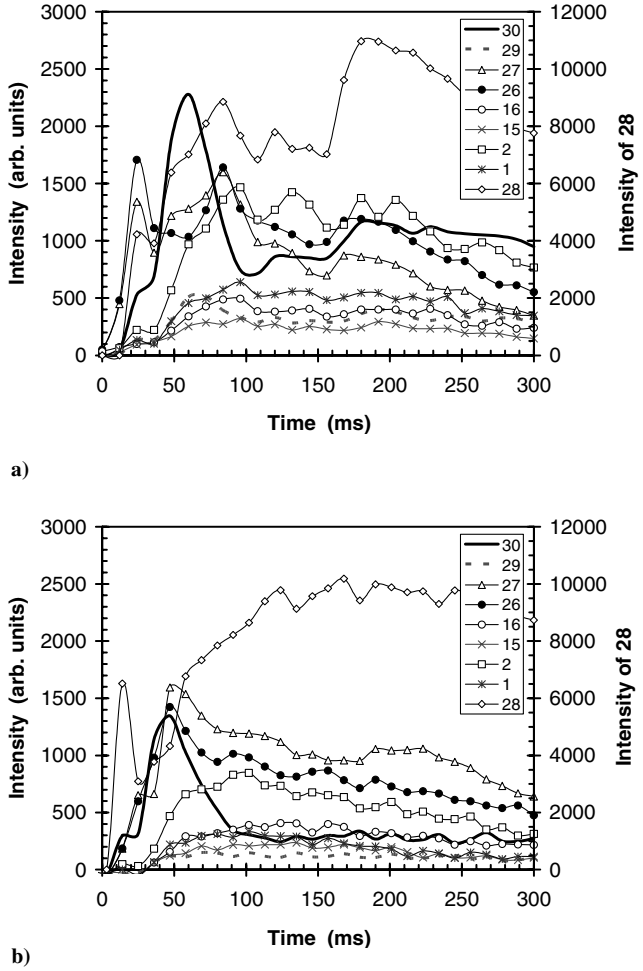

Fig. 14 Species from recombined plasma (5 kV Lexan) and decomposed propellants: a) JA2 and b) M43.

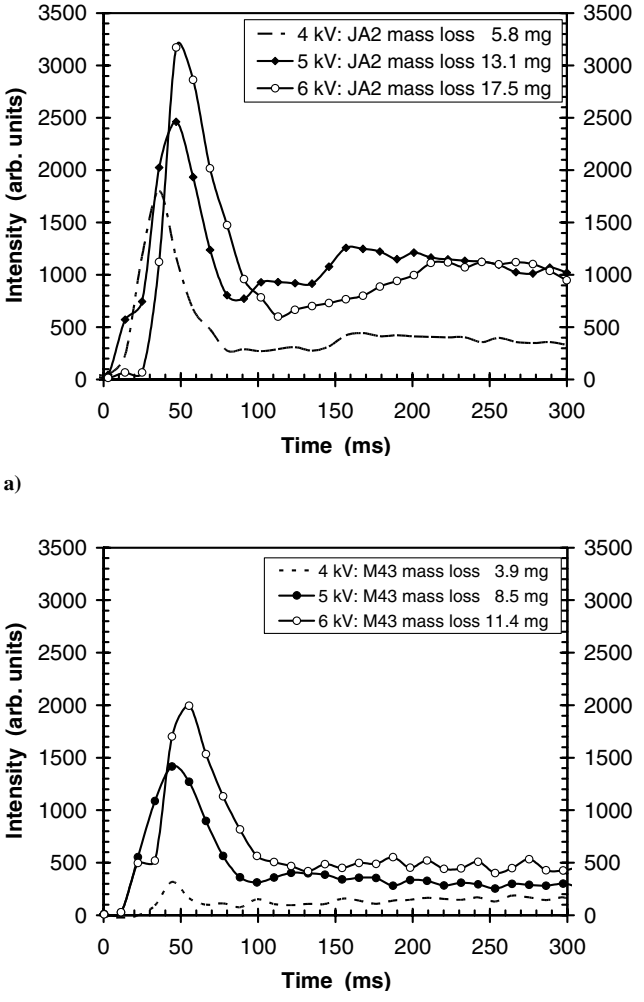

Fig. 15 Effect of plasma energy on the yield of mass 30 from decomposition of a) JA2 and b) M43.

ingredients were consistently detected for both propellants, which are NO and HCO, the latter being a fragment of H_2CO resulting from electron impact in the ionizer [24]. It is also possible that ignition and combustion of part of the propellant sample (the ablated mass) were achieved during its interaction with the jet, because NO and H_2CO are typical "dark zone" and final products observed from JA2 combustion [25]. However, Beyer and Pesce-Rodriguez [26] used Fourier transform infrared spectroscopy to analyze JA2 decomposition products induced by plasma radiation only and found no detectable oxides of nitrogen but showed the presence of CO_2 and CO. This may also suggest that ignition of the ablated mass of the propellant is achieved during sampling in this work.

It is noted that NO is also seen in tests with no propellant due to the interaction of plasma with air in the holding chamber, but in that case, its intensity is very small. Clearly, in tests with propellants, NO primarily comes from the propellants. Therefore, it is expected that the intensity of NO should increase as more amount of propellant decomposes. This was verified with the measurement of mass loss of the propellant after exposure to the plasma. The results are presented in Fig. 15, which indicate that more propellant mass loss at higher plasma energies gives higher intensity of NO for both propellants. At the same energy level, a smaller amount of mass was lost from M43 compared with that from JA2, resulting in the difference in NO intensities detected.

Summary and Conclusions

Experiments were conducted using a triple-quadrupole molecular beam mass spectrometer to measure species from ETC plasma during recombination and from decomposition of propellants (JA2 and M43) exposed to the plasma. The mismatch between the plasma pulse duration and the sampling time requirement by the mass spectrometer makes direct probing plasma species impossible, so a plasma-holding chamber was used to prolong the event for sampling. The secondary jet evolving from the holding chamber should represent the nature of the plasma as it propagates through the propellant bed in actual ETC applications. Parameters varied during the experiments include capillary material, plasma energy level, and initial background conditions. Results show that when the plasma cools, recombination of its initial species takes place rapidly. Recombination species that can be consistently detected are C_2H_4, C_2H_3, C_2H_2, CH_4, CH_3, H_2, and H for PE plasma. When sufficient air is present in the chamber or using Lexan capillary, NO, CO, and CO_2 are also detectable. Another major product from plasma recombination is soot, which consistently appears in considerable amounts under all conditions for both Lexan plasma and PE plasma. Plasma-induced decomposition of JA2 and M43 indicated the formation of NO and H_2CO, which are typical "dark-zone" species observed for these propellants suggesting ignition and combustion of lost masses of the propellants.

Acknowledgments

This work was performed under the sponsorship of the Army Research Office, Contract DAAD19-03-1-0340. The support and encouragement of D. M. Mann are greatly appreciated. Also the authors wish to acknowledge J. Yu at Alliant Techsystems—Radford Army Ammunition Plant for the shipment of JA2 propellant.

References

[1] Oberle, W. F., and Wren, G. P., "Ballistic Efficiency of Electrical Energy in ETC Propulsion Concepts," *Proceedings of the 32nd JANNAF Combustion Meeting*, CPIA Publication 631, Vol. 1, Johns Hopkins Univ., Baltimore, MD, 1995, pp. 47–58.

[2] Bourham, M. A., Gilligan, J. G., and Oberle, W. F., "Analysis of Solid Propellant Combustion Behavior under Electrothermal Plasma Injection for ETC Launchers," *IEEE Transactions on Magnetics*, Vol. 33, No. 1, 1997, pp. 278–283.

[3] Perelmutter, L., Sudai, M., Goldenberg, C., Kimhe, D., Zeevi, Z., Arie, S., Melnik, M., and Melnik, D., "Plasma Propagation and Ignition in the Chamber of a SPETC Gun," *IEEE Transactions on Magnetics*, Vol. 35, No. 1, 1999, pp. 213–217.

[4] Nusca, M. J., McQuaid, M. J., and Anderson, W. R., "Development and Validation of a Multi-Species Reacting Flow Model for the Plasma Jet Generated by an ETC Igniter," *Proceedings of the 37th JANNAF Combustion Subcommittee Meeting*, CPIA Publication 701, Vol. 1, Johns Hopkins Univ., Baltimore, MD, 2000, pp. 181–199.

[5] Li, J.-Q., Zhou, H., Kudva, G., Thynell, S., and Litzinger, T., "Experimental Investigation of Plasma Propellant Interactions," *Proceedings of 37th JANNAF Combustion Subcommittee Meeting*, CPIA Publication 701, Vol. 1, Johns Hopkins Univ., Baltimore, MD, 2000, pp. 109–121.

[6] Taylor, M. J., "Ignition of Propellant by Metallic Vapour Deposition for an ETC Gun System," *Propellants, Explosives, Pyrotechnics*, Vol. 26, No. 3, 2001, pp. 137–143.

[7] Kim, J. U., Clemens, N. T., and Varghese, P. L., "Experimental Study of the Transient Underexpanded Jet Generated by Electrothermal Capillary Plasma," *Journal of Propulsion and Power*, Vol. 18, No. 6, 2002, pp. 1153–1160.

[8] Beyer, R. A., and Pesce-Rodriguez, R. A., "Experiments to Define Plasma-Propellant Interactions," *IEEE Transactions on Magnetics*, Vol. 39, No. 1, 2003, pp. 207–211.

[9] Katulka, G. L., and Dyvik, J. A., "Experimental Results of Electrical Plasma Ignition in 120-mm Solid Propellant Tank Gun Firings," *Proceedings of the 33rd JANNAF Combustion Meeting*, CPIA Publication 653, Vol. 3, Johns Hopkins Univ., Baltimore, MD, 1996, pp. 103–110.

[10] Marinos, C., "ETC Ignition and Temperature Sensitivity," *Proceedings of the 32nd JANNAF Combustion Meeting*, CPIA Publication 631, Vol. 3, Johns Hopkins Univ., Baltimore, MD, 1995, pp. 109–118.

[11] Dyvik, J. A., and Katulka, G. L., "ETC Temperature Compensation: Experimental Results of 120-mm Test Firings," *Proceedings of the 33rd JANNAF Combustion Meeting*, CPIA Publication 653, Vol. 1, Johns Hopkins Univ., Baltimore, MD, 1996, pp. 111–119.

[12] Del Guercio, M., "Propellant Burn Rate Modification by Plasma Injection," *Proceedings of the 34th JANNAF Combustion Meeting*, CPIA Publication 662, Vol. 1, Johns Hopkins Univ., Baltimore, MD, 1997, pp. 35–42.

[13] Chaboki, A., Zelenak, S., and Isle, B., "Recent Advances in Electrothermal-Chemical Gun Propulsion at United Defense, L. P.," *IEEE Transactions on Magnetics*, Vol. 33, No. 1, 1997, pp. 284–288.

[14] Wren, G. P., and Oberle, W. F., "Influence of High Loading Density Charge Configurations on Performance of Electrothermal-Chemical (ETC) Guns," *IEEE Transactions on Magnetics*, Vol. 37, No. 1, 2001, pp. 211–215.

[15] Perelmutter, L., Sudai, M., Goldenberg, C., Kimhe, D., Zeevi, Z., Arie, S., Melnik, M., and Melnik, D., "Plasma Propagation and Ignition in the Chamber of a SPETC Gun," *IEEE Transactions on Magnetics*, Vol. 35, No. 1, 1999, pp. 213–217.

[16] Li, J.-Q., "A Study of an Electrothermal Plasma and its Interaction with Propellants," Ph.D. Dissertation, Mechanical and Nuclear Engineering Dept., The Pennsylvania State University, University Park, PA, May 2004.

[17] Li, J.-Q., Litzinger, T. A., and Thynell, S. T., "Interactions of Capillary Plasma with Double-Base and Composite Propellants," *Journal of Propulsion and Power*, Vol. 20, No. 4, 2004, pp. 675–683.

[18] Li, J.-Q., Litzinger, T. A., and Thynell, S. T., "Plasma Ignition and Combustion of JA2 Propellant," *Journal of Propulsion and Power*, Vol. 21, No. 1, 2005, pp. 44–53.

[19] Li, J.-Q., Litzinger, T. A., Das, M., and Thynell, S. T., "Study of Plasma-Propellant Interaction During Normal Impingement," *Journal of Propulsion and Power*, 2005 (to be published).

[20] McQuaid, M. J., and Nusca, M. J., "Calculating the Chemical Compositions of Plasmas Generated by an Ablating-Capillary Arc Ignition System," *Proceedings of the 36th JANNAF Combustion Subcommittee Meeting*, CPIA Publication 691, Vol. 2, Johns Hopkins Univ., Baltimore, MD, 1999, pp. 133–142.

[21] Kohel, J. M., Su, L. K., Clemens, N. T., and Varghese, P. L., "Emission Spectroscopic Measurements and Analysis of a Pulsed Plasma Jet," *IEEE Transactions on Magnetics*, Vol. 35, No. 1, 1999, pp. 201–206.

[22] "Species Data: Mass Spectrum," *NIST Chemistry WebBook* [online database], http://webbook.nist.gov/chemistry [cited 28 April 2005].

[23] Nusca, M. J., and McQuaid, M. J., "Modeling the Open-Air Plasma Jet From an ETC Igniter Using a Multi-Species Reacting Flow CFD Code," *Proceedings of the 36th JANNAF Combustion Subcommittee Meeting*, CPIA Publication 691, Vol. 2, Johns Hopkins Univ., Baltimore, MD, 1999, pp. 143–157.

[24] Lee, Y. J., "A Study of the Chemical and Physical Processes Governing CO2 Laser-Induced Pyrolysis and Combustion of RDX, BAMO, and RDX/BAMO Pseudo-Propellants," Ph.D. Dissertation, Mechanical and Nuclear Engineering Dept., The Pennsylvania State University, University Park, PA, May 1996.

[25] Fifer, R. A., "Chemistry of Nitrate Ester and Nitramine Propellants," *Fundamentals of Solid-Propellant Combustion*, edited by Kuo, K. K., and Summerfield, M., AIAA, New York, 1984, Chap. 4, pp. 177–237.

[26] Beyer, R. A., and Pesce-Rodriguez, R. A., "The Response of Propellants to Plasma Radiation," *IEEE Transactions on Magnetics*, Vol. 41, No. 1, 2005, pp. 344–349.

M. Brewster
Associate Editor